87-fs mode-locked Tm,Ho:CaYAlO$_4$ laser at ~2043 nm

Yongguang Zhao,[1,2,*] Yicheng Wang,[1] Xuzhao Zhang,[3] Xavier Mateos,[3] Zhongben Pan,[1,4] Pavel Loiko,[5] Wei Zhou[2], Xiaodong Xu,[2] Ju Xu,[6] Deyuan Shen,[2] Soile Suomalainen,[7] Antti Härkönen,[7] Mircea Guina,[7] Uwe Griebner,[1] and Valentin Petrov[1]

[1]*Max-Born-Institute for Nonlinear Optics and Short Pulse Spectroscopy, Max-Born-Str. 2a, D-12489 Berlin, Germany*
[2]*Jiangsu Key Laboratory of Advanced Laser Materials and Devices, Jiangsu Normal University, 221116 Xuzhou, China*
[3]*Física i Cristal·lografia de Materials i Nanomaterials (FiCMA-FiCNA), Universitat Rovira i Virgili (URV), Campus Sescelades, c/ Marcel·lí Domingo, s/n., E-43007 Tarragona, Spain*
[4]*Institute of Chemical Materials, China Academy of Engineering Physics, 621900 Mianyang, China*
[5]*ITMO University, 49 Kronverkskiy pr., 197101 St. Petersburg, Russia*
[6]*School of Physics Science and Engineering, Institute for Advanced Study, Tongji University, 200092 Shanghai, China*
[7]*Optoelectronics Research Centre, Tampere University of Technology, PO Box 692, 33101 Tampere, Finland*
**Corresponding author: Yongguangzhao@yeah.net*

Received XX Month XXXX

We report on the first sub-100-fs mode-locked Ho^{3+}-laser in the 2-µm spectral range employing a disordered co-doped Tm,Ho:CaYAlO$_4$ (Tm,Ho:CALYO) crystal as a gain medium. Pulses as short as 87 fs are produced with an average output power of 27 mW at 80.45-MHz repetition rate. An output power of 96 mW is reached for a pulse duration of 98 fs.

OCIS codes: *(140.4050) Mode-locked lasers; (140.3380) Laser materials; (140.3580) Lasers, solid-state; (140. 3070); Infrared and far-infrared lasers.*

http://dx.doi.org/10.1364/OL.99.099999

Ultrafast solid-state lasers emitting around 2 µm are in the focus of recent laser research owing to their potential applications in Lidar, time-resolved spectroscopy, atmospheric remote-sensing, optical communications, and medicine, etc. Crystalline, ceramic and glass materials doped with Thulium (Tm^{3+}) and/or Holmium (Ho^{3+}) ions are currently the most promising candidates for such laser sources. To date, pulses as short as 86 fs have been generated with a graphene mode-locked Tm:MgWO$_4$ bulk laser at a central wavelength of 2017 nm [1]. In comparison, steady-state passive mode-locking of Ho^{3+}-doped materials which are characterized by slightly longer emission wavelength and approximately 5 times higher cross section [2], resulted in longer pulse durations [3-9]. This has been attributed to the structured emission spectrum [10,11]. Exploiting disordered laser hosts can profit from inhomogeneous spectral line broadening of the doped active ion emission which is primarily determined by the electronic structure but can be modulated by the crystal field of the host materials. The effect is expected to be more pronounced for dopant ions which exhibit less electron-phonon coupling, such as Nd^{3+} or Ho^{3+}, as compared to Yb^{3+} [12] and is also expected to smooth the spectral features. Thus, the ordered Tm,Ho:KY(WO$_4$)$_2$ single crystal generated transform-limited 570-fs pulses [7] while the chemically related but structurally different disordered Tm,Ho:NaY(WO$_4$)$_2$ generated pulses as short as 191 fs by essentially the same mode-locking technique (semiconductor saturable absorber mirror, SESAM) [8].

Recently, the ABCO$_4$-type oxide crystals, where A is either Ca or Sr, B is Y or Ln, and C is Al or Ga, were proved to be excellent hosts with broadened emission spectra of the doped active ions, which is favorable for ultrashort pulse generation. They belong to the tetragonal crystal system (space group $I4/mmm$ or D_{4h}^{17}, point group $4/mmm$). A and B statistically occupy the same 9-fold O^{2-}-coordinated site with tetragonal $4mm$ local symmetry whereas C is in octahedral sites. Pulses as short as 40 fs were demonstrated in the 1 µm spectral range using Yb^{3+}:CaGdAlO$_4$ (Yb:CALGO) [13], as well as 30 fs using Yb^{3+}:CaYAlO$_4$ (Yb:CALYO) laser, the shortest pulses ever reported for mode-locked Yb bulk lasers [14].

Similar to Yb^{3+}, the Tm^{3+} ions (ionic radius: 1.052 Å) replace the Gd^{3+}/Y^{3+} ones which have a closer radius (1.107 Å/1.110 Å) compared to the Ca^{2+} ions (1.180 Å). The local disorder affecting the crystal field for Tm^{3+} originates from the second coordination sphere of the Ca^{2+}-Gd^{3+}/Y^{3+} ions due to the charge difference of these two ions and the different cation-cation distances [15]. However, in the 2 µm spectral range, the shortest pulses produced by mode-locked Tm:ABCO$_4$ lasers were ~650 fs due to the effect of water absorption peaks [16]. By co-doping with Ho^{3+} ions, the gain spectrum will tune to slightly longer wavelengths where air absorption and the associated dispersion will not be detrimental, and one could utilize the potential of the disordered ABCO$_4$ hosts.

In this work, we demonstrate a stable, self-starting Tm,Ho:CALYO mode-locked laser by applying a GaSb-based SESAM and chirped mirrors (CMs) for dispersion management. Nearly Fourier-limited pulses as short as 87 fs with a corresponding spectral bandwidth of 56.3 nm centered at 2042.6 nm are achieved.

Preliminary spectroscopic characteristics of Tm,Ho:CALYO have been already reported [17,18]. The maximum absorption coefficient is around 795 nm with a full width at half maximum (FWHM) of more than 18 nm [17]. The emission due to the $^3F_4 \rightarrow {}^3H_6$ transition in Tm^{3+} together with the $^5I_7 \rightarrow {}^5I_8$ transition in Ho^{3+} extends from 1600 to 2200 nm, with the fluorescence lifetime of 5.47 and 7.63 ms [18], respectively.

Figure 1 shows the schematic of the Tm,Ho:CALYO continuous wave (CW) and mode-locked lasers. The Tm,Ho:CALYO crystal (6.24 at.% Tm^{3+}, 1.25 at.% Ho^{3+}) was cut along the a-axis (thickness: 3.1 mm) with an aperture of 3(a) × 3(c) mm^3. Both end faces were anti-reflection (AR) coated for the pump and laser wavelengths so that it could be used at normal incidence. To mitigate the thermal load, the crystal was tightly mounted in a copper holder and water cooled to 14.0 °C. The pump source was a wavelength tunable Ti:sapphire laser with a maximum output power of 3.6 W at 795.3 nm. The collimated pump light was focused by an AR-coated lens (f=70 mm) and incident onto the crystal with a beam diameter of ~ 60 μm. The standard X-folded cavity consisted of M$_1$, M$_2$ (plano-concave mirrors, radius of curvature RoC = - 100 mm), M$_3$ (plane mirror), and OC (output coupler). The transmission T of the used OCs was 0.2%, 0.5%, 1.5%, and 3%. A 3-mm thick quartz plate was employed as a Lyot-filter for wavelength tuning. The GaSb-based SESAM used as a saturable absorber contained two quantum wells and was uncoated [19]. In order to ensure the required fluence for saturation of the SESAM, a second beam waist with a diameter of ~ 160 μm was created using a plano-concave chirped mirror CM$_3$ (RoC = - 100 mm). In addition, chirped mirrors CM$_1$-CM$_2$, CM$_4$-CM$_5$ were respectively inserted into the two arms of the cavity to perform the dispersion management.

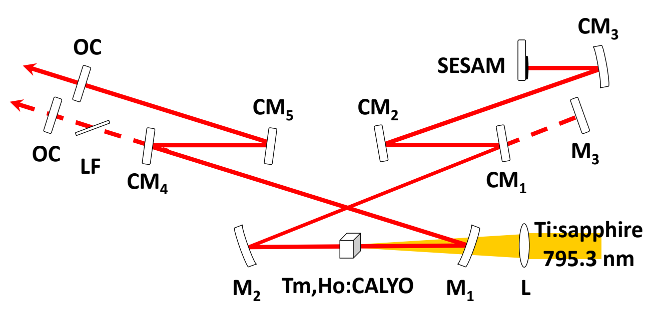

Fig. 1. Scheme of the CW and mode-locked Tm,Ho:CALYO laser. (L, lens; CM$_1$-CM$_5$, chirped mirrors; M, mirrors, OC, output coupler, LF, Loyt-Filter)

First, the Tm,Ho:CALYO laser was operated in the CW regime without the CMs and the SESAM. The cavity was nearly symmetric with a total length of about 1.5 m. With increasing the pump power, the crystal absorption (measured under lasing conditions with the 1.5% OC) decreased from 95.6% to 87.6% for π-polarization ($E//c$), and from 77.2% to 70.4% for σ-polarization ($E//a$), due to absorption bleaching under tight focusing. The measured maximum absorbed pump power was 2.44 W for σ-polarized pumping and 3.05 W for π-polarization. The corresponding output power is shown in Fig. 2 for the different OCs. A maximum output power of 0.95 W was obtained with T= 1.5%, corresponding to a slope efficiency of 32.7% for π pump polarization. Further power increase was limited by the available pump power but the linear dependence indicates the potential for power scaling. The σ pump polarization provided similar slope efficiencies but the output power was restricted due to the lower absorption. The reduction of the slope efficiency for T = 3% is attributed to excited state interactions at higher population of the upper laser level.

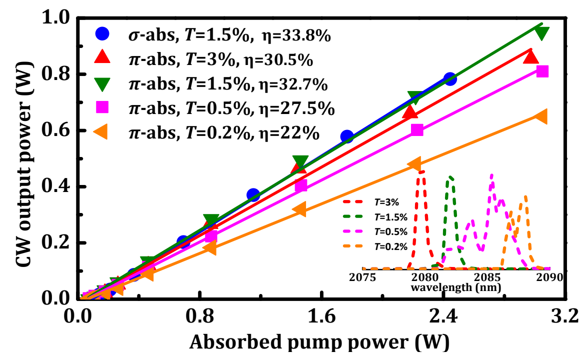

Fig. 2. CW input-output performance of the Tm,Ho:CALYO laser for different OCs and pump polarization. η is the slope efficiency with respect to the absorbed power. The inset shows the laser spectra recorded for π-polarized pump. The laser polarization is always π.

A Glan prism was employed to measure the polarization properties of the laser beam, which was naturally selected by the uniaxial Tm,Ho:CALYO crystal [17]. It was found to be linearly polarized and always π, independent of the pump polarization, with a polarization extinction ratio (PER) as high as 21 dB, indicating higher gain cross-section for this polarization. The laser spectra recorded for different OCs (see inset of Fig. 2), indicate a red shift of the central wavelength from 2079.5 to 2088 nm when decreasing the transmission of the OCs. Such a red shift is characteristic of quasi-three-level laser systems and attributed to the lower required population inversion ratio for laser oscillation at lower T, which results in stronger reabsorption effect.

With the Loyt-filter in the cavity, the laser was tunable over 115 nm, i.e. from 1970 to 2085 nm. As shown in Fig. 3(a), the output power increased with the laser wavelength, however, it rapidly dropped above 2085 nm due to the dramatic increase of the OC transmission and thereby a larger loss. The tuning curve of the Tm,Ho:CALYO laser has a similar profile to its fluorescence spectrum in which Tm^{3+} and Ho^{3+} emission overlap [17,18]. Thus, lasing above 1995 nm is attributed to Ho^{3+} while at shorter wavelengths it is due to Tm^{3+}. In addition, the lower power of the Tm^{3+} emission indicates that the concentration of Ho^{3+} ions is high enough to accept the energy transferred from the excited Tm^{3+} ions [18].

One notable feature of this laser was the strong visible luminescence resulting from up-conversion processes in both Tm^{3+} and Ho^{3+} ions, which inevitably reduces the population in the upper laser levels, and thereby the laser efficiency [20]. The spectral distribution of the measured up-conversion luminescence is shown in Fig. 3(b) on a logarithmic scale. Three peaks located at 478, 546 and 651 nm were observed, which correspond to the transitions $^1G_4 \rightarrow {}^3H_6$ (Tm^{3+}), $^5F_4,{}^5S_2 \rightarrow {}^5I_8$ (Ho^{3+}), and $^1G_4 \rightarrow {}^3F_4$ in (Tm^{3+}) + $^5F_5 \rightarrow {}^5I_8$ (Ho^{3+}) [21]. Obviously, the strongest up-conversion occurs for the $^5F_4,{}^5S_2 \rightarrow {}^5I_8$ transition in Ho^{3+}, which means that the laser performance might be further improved by appropriately reducing the Ho-doping concentration [20,22].

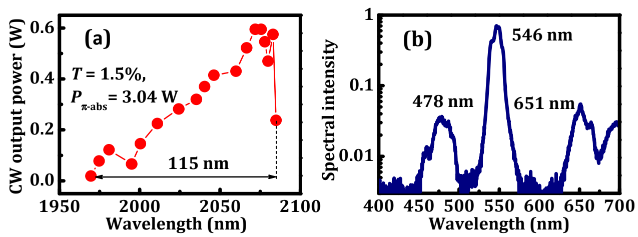

Fig. 3. (a) Tunability of the CW Tm,Ho:CALYO laser at 3.05 W absorbed pump power and (b) up-conversion luminescence spectrum under 795.3 nm excitation.

Mode-locking was studied with the CMs and the GaSb-based SESAM inserted into the cavity, leading to a total physical cavity length of about 1.86 m. The group delay dispersion (GDD) of the CMs was -125 fs^2 per bounce. Taking into account the group velocity dispersion (GVD) of the CALYO crystal, appr. -56 fs^2/mm at 2040 nm [23], the total round trip GDD amounted to -1550 fs^2 (see Fig. 4(a)). Increasing the pump power, the Tm,Ho:CALYO laser switched from the CW regime to self-starting mode-locking. With T = 1.5%, the threshold for mode-locking was at an absorbed power of about 0.85 W. The central wavelength was 2077.6 nm and the average output power reached 268 mW at the maximum pump level. The spectral width (FWHM) and the pulse duration (FWHM assuming sech^2-intensity profile) amounted to 11.8 nm and 412 fs, respectively. By further adjusting the separation between M_1 and M_2, another stable mode-locking region with shorter pulse duration but lower output power was found for the same cavity. In this case, the maximum average output power reached 96 mW, corresponding to a single pulse energy of 1.2 nJ and ~400 μJ/cm^2 average intracavity fluence on the SESAM. The self-starting mode-locked Tm,Ho:CALYO laser was very stable and no multi-pulsing or satellites were observed. As shown by the blue line in Fig. 4 (a), the laser wavelength was 2032 nm and the spectral FWHM amounted to 46.6 nm. The corresponding pulse duration (FWHM) was 98 fs which gives a time-bandwidth product (TBP) of $\Delta\nu\tau$ = 0.332 (see Fig. 4(c)). Similar to the situation observed with the Tm,Ho:NaY$(WO_4)_2$ mode-locked laser described in [7], the second shorter pulse generation regime can be attributed to enhanced self-phase modulation (SPM) in the gain medium as a result of the tighter mode focusing conditions. However, pure Kerr-lens mode-locking was not observed in the absence of SESAM in the cavity, which indicates that the SESAM was instrumental for initiation and initial pulse shaping while SPM was the primary mechanism enabling sub-100-fs pulse generation. Moreover, in the present experiment, the blue shift of the central wavelength from 2077.6 nm (where the laser has a higher gain as shown in Fig. 3(a)) to 2032 nm was a result of the combined action of SPM and the cut-off above ~2100 nm of the cavity mirror reflectivities (in particular the OC).

In order to further shorten the pulse duration, we employed an OC with lower transmission, T = 0.2%. As expected, the laser initially ran in the longer pulse mode-locking regime with the following output characteristics: pulse duration of 233 fs at a maximum average power of 156 mW, central wavelength of 2080.6 nm and spectral FWHM of 20.4 nm. Similarly, additional alignment of the cavity produced substantially shorter pulses with this OC but in this case the maximum absorbed pump power for stable operation was 2.74 W. This limitation is attributed to the higher intracavity intensity. At this maximum pump level the average output power reached 27 mW, corresponding to an average fluence of ~800 μJ/cm^2 on the SESAM. The corresponding optical spectrum is shown by the red line in Fig. 4(a). The central wavelength is 2042.6 nm and the FWHM amounts to 56.3 nm, larger compared to the T = 1.5% case. The red shift of the wavelength can be attributed to the decreased population inversion as in the case of the CW laser. The multi-sideband observed at longer wavelengths is considered to be an artefact due to the increasing transmission of the OC. In the peak at 2184 nm, the transmission of this OC increases to 10% (i.e. 50 times). The leakage exhibits, however, some structure which cannot be associated with the measured OC characteristics. It might be related to impulsive Raman scattering in the gain medium [24]. Figure 4(b) shows the measured spontaneous Raman spectrum (a(ππ)a) of the Tm,Ho:CALYO crystal, where the Raman line at 321 cm^{-1} exactly corresponds to the spectral shift from the maximum of the optical spectrum at 2041 nm to 2184 nm.

Figure 4(d) shows the corresponding intensity autocorrelation trace from which a pulse duration of 87 fs is derived. The resulting TBP is $\Delta\nu\tau$ = 0.352, close to the Fourier-limit for sech^2-shaped pulses. Moreover, single clean pulse operation was confirmed by checking the autocorrelation intensity on a longer time scale of ±6.5 ps.

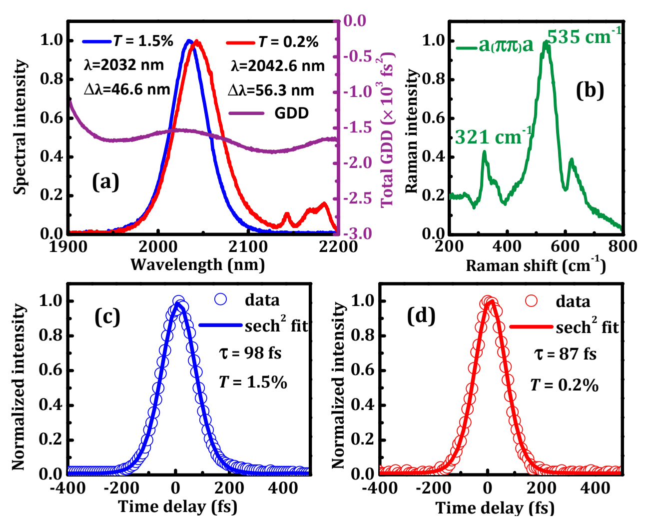

Fig. 4. (a) Optical spectra and (c), (d) the corresponding intensity autocorrelation traces of the mode-locked Tm,Ho:CALYO laser with T= 1.5% and 0.2%. (b) Raman spectrum of the Tm,Ho:CALYO crystal for the $a(\pi\pi)a$ configuration (Porto's notation).

To further characterize the stability of the mode-locked Tm,Ho:CALYO laser for the shortest pulse durations, radio frequency (RF) spectra were recorded with a fast InGaAs photodiode and a spectrum analyzer. Figure 5 shows the RF spectrum of the fundamental beat note at 80.45 MHz recorded with 100 Hz resolution bandwidth (RBW) and 300 kHz span. The extinction ratio of 79 dBc above the noise level is indicative of stable steady-state mode-locking. The inset shows the RF spectrum recorded in a 2 GHz span with 300-kHz RBW: The uniform harmonic beat notes and the absence of spurious modulations present further evidence for stable and clean mode-locked regime of the Tm,Ho:CALYO laser.

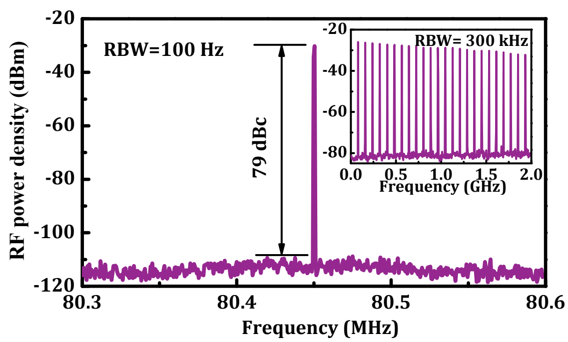

Fig. 5. Radio frequency spectrum of the mode-locked Tm,Ho:CALYO laser: fundamental beat note (inset: 2 GHz span, RBW: resolution bandwidth).

In conclusion, we have experimentally demonstrated CW and first passively mode-locked operation of a Tm,Ho:CALYO laser. For the naturally selected π-polarization the Tm,Ho:CALYO laser produced an output 0.95 W in the CW regime without any roll-off. Operation above 2 µm without any spectrally selective elements is a prerequisite for femtosecond pulse generation. By exploiting the broad and smooth spectral emission of Ho^{3+} in the disordered CALYO crystal, sub-100 fs pulses were achieved. With T = 1.5%, a maximum average output power of 96 mW was obtained for a pulse duration of 98 fs. Reducing the OC transmission to increase the intracavity intensity and enhance the SPM in the gain medium, nearly transform-limited 87-fs pulses were produced with 27-mW average output power. To the best of our knowledge these are the shortest pulses from mode-locked Ho^{3+} lasers in the 2 µm spectral range, including singly Ho-doped or Tm,Ho co-doped bulk and fiber lasers.

The achieved sub-100 fs pulse durations practically reproduce the best results demonstrated with passively mode-locked Tm-lasers [1]. The longer emission wavelength is, however, more promising for further pulse shortening through SPM and soliton-like shaping since air absorption is less pronounced. A further step in this direction will require cavity mirrors with extended long wave reflectivity. In addition, the photoluminescence of the GaSb-based SESAM used in the present work was located around 2060 nm [19], not matched to the maximum gain at 2080-2090 nm. Graphene with its wavelength independence [1,25] might turn out advantageous for operation at such long wavelengths.

Besides the already mentioned optimization of the doping levels, the CALYO and the related CALGO disordered crystals could prove very attractive for ultrashort pulse generation also with single Ho-doping under in-band resonant pumping into the upper laser level [7,26]. Some parasitic processes can be avoided in this simpler system while the greatly reduced heat generation could provide a route towards power scaling.

Funding. National Natural Science Foundation of China (NSFC) (61505072, 51402268); Natural Science Foundation of Jiangsu Province, China (BK20150240).

REFERENCES

1. Y. Wang, W. Chen, M. Mero, L. Zhang, H. Lin, Z. Lin, G. Zhang, F. Rotermund, Y. J. Cho, P. Loiko, X, Mateos, U. Grierbner, and V. Petrov, Opt. Lett. **42,** 3076 (2017).
2. S. A. Payne, L. L. Chase, L. K. Smith, W. L. Kway, and W. F. Krupke, IEEE J. Quantum Electron. **28**, 2619 (1992).
3. F. Heine, E. Heumann, G. Huber, and K. L. Schepler, Appl. Phys. Lett. **60**, 1161 (1992).
4. N. Coluccelli, A. Lagatsky, A. D. Lieto, M. Tonelli, G.Galzerano, W. Sibbett, and P. Laporta, Opt. Lett. **36**, 3209 (2011).
5. A. Lagatsky, F. Fusari, S. Calvez, J. A. Gupta, V. E. Kisel, N. V. Kuleshov, C. T.A. Brown, M. D. Dawson, and W. Sibbett, Opt. Lett. **34**, 2587 (2009).
6. Y. Wang, R. Lan, X. Mateos, J. Li, C. Hu. C. Li, Y. Pan, S. Suomalainen, A. Härkönen, M. Guina, V. Petrov, and U. Griebner, Opt. Express **24**, 18003 (2016).
7. A. A. Lagatsky, F. Fusari, S. Calvez, S. V. Kurilchik, V. E. Kisel, N. V. Kuleshov, M. D. Dawson, C. T. A. Brown, and W. Sibbett, Opt. Lett. **35**, 172 (2010).
8. A. A. Lagatsky, X. Han, M. D. Serrano, C. Cascales, C. Zaldo, S. Calvez, M. D. Dawson, J. A. Gupta, C. T. A. Brown, and W. Sibbett, Opt. Lett. **35,** 3027 (2010).
9. J. Zhang, K. F. Mak, S. Gröbmeyer, D. Bauer, D. Sutter, V. Pervak, F. Krausz, and O. Pronin, Conference on Lasers and Electro-Optics 2017 (Optical Society of America), paper SM1I.6.
10. E. P. Chicklis, C. S. Naiman, R. C. Folweiler, and J. C. Doherty, IEEE J. Quantum Electron. **8**, 225 (1972).
11. K. L. Nash, R. C. Dennis, N. J. Ray, J. B. Gruber, and D. K. Sardar, J. Appl. Phys. **106**, 063117 (2009).
12. Y. Zhao, H. Yu, Z. Wang, H. Zhang, X. Xu, and J. Wang, J. Opt. Soc. Am. B **30**, 1241 (2013).
13. A. Agnesi, A. Greborio, F. Pirzio, G. Reali, J. A. Au, and A. Guandalini, Opt. Express **20**, 10077 (2012).
14. J. Ma, H, Huang, K. Ning, X. Xu, G. Xie, L. Qian, K. P. Lon, and D. Tang, Opt. Lett. **41**, 890 (2016).
15. P. O. Petit, J. Petit, P. Goldner, and B. Viana, Opt. Mater. **30**, 1093 (2008).
16. Y. Wang, G. Xie, X. Xu, J. Di, Z. Qin, S. Suomalainen, M. Guina, A. Härkönen, A. Agnesi, U. Griebner, X. Mateos, P. Loiko, and V. Petrov, Opt. Mater. Express **6**, 131 (2015).
17. J. Q. Di, D. H. Zhou, X. D. Xu, C. T. Xia, W. Gao, H. R. Zheng, Q. L. Sai, F. Mou, and J. Xu, Cryst. Res. Technol. **49**, 446 (2014).
18. S. F. Gao, Z. Y. You, J. L. Xu, Y. J. Sun, and C. Y. Tu, Mater. Lett. **141**, 59 (2015).
19. J. Paajaste, S. Suomalainen, A. Härkönen, U. Griebner, G. Steinmeyer, and M. Guina, J. Phys. D: Appl. Phys. **47**, 065102 (2014).
20. G. Rustad and K. Stenersen, IEEE J. Quantum Electron. **32**, 1645 (1996).
21. N. K. Giri, D. K. Rai, and S. B. Rai, J. Appl. Phys. **104**, 113107 (2008).
22. J. H. Chung, J. H. Ryu, S. W. Mhin, K. M. Kim, and K. B. Shim, J. Mater. Chem. **22,** 3997 (2012).
23. P. Loiko, P. Becker, L. Bohatý, C. Liebald, M. Peltz, S. Vernay, D. Rytz, J. M. Serres, X. Mateos, Y. Wang, X. Xu, J. Xu, A. Major, A. Baranov, U. Griebner, and V. Petrov, Opt. Lett. **42**, 2275 (2017).
24. Y. Ishida, K. Naganuma, and H. Kamada, Opt. Rev. **6**, 37 (1999).
25. Z. Sun, T. Hasan, F. Torrisi, D. Popa, G. Privitera, F. Wang, F. Bonaccorso, D. M. Basko, and A. C. Ferrari, ACS Nano **4**, 803 (2010).
26. M. Schellhorn, D. Parisi, M. Eichhorn, and M. Tonelli, Opt. Lett. **39**, 1193 (2014).

REFERENCES

1. Y. Wang, W. Chen, M. Mero, L. Zhang, H. Lin, Z. Lin, G. Zhang, F. Rotermund, Y. J. Cho, P. Loiko, X, Mateos, U. Grierbner, and V. Petrov, “Sub-100 fs Tm:$MgWO_4$ laser at 2017 nm mode locked by a graphene saturable absorber,” Opt. Lett. **42,** 3076-3079 (2017).
2. S. A. Payne, L. L. Chase, L. K. Smith, W. L. Kway, and W. F. Krupke, “Infrared cross-section measurements for crystals doped with Er^{3+}, Tm^{3+}, and Ho^{3+},” IEEE J. Quantum Electron. **28**, 2619-2630 (1992).
3. F. Heine, E. Heumann, G. Huber, and K. L. Schepler, "Mode locking of room-temperature cw thulium and holmium lasers," Appl. Phys. Lett. **60**, 1161-1162 (1992).
4. N. Coluccelli, A. Lagatsky, A. D. Lieto, M. Tonelli, G.Galzerano, W. Sibbett, and P. Laporta, “Passive mode locking of an in-band-pumped Ho:$YLiF_4$ laser at 2.06 µm,” Opt. Lett. **36**, 3209-3211 (2011).
5. A. Lagatsky, F. Fusari, S. Calvez, J. A. Gupta, V. E. Kisel, N. V. Kuleshov, C. T.A. Brown, M. D. Dawson, and W. Sibbett, “Passive mode locking of a Tm,Ho:$KY(WO_4)_2$ laser around 2 µm,” Opt. Lett. **34**, 2587-2589 (2009).
6. Y. Wang, R. Lan, X. Mateos, J. Li, C. Hu. C. Li, Y. Pan, S. Suomalainen, A. Härkönen, M. Guina, V. Petrov, and U. Griebner, “Broadly tunable mode-locked Ho:YAG ceramic laser around 2.1 µm,” Opt. Express **24**, 18003-18012 (2016).
7. A. A. Lagatsky, F. Fusari, S. Calvez, S. V. Kurilchik, V. E. Kisel, N. V. Kuleshov, M. D. Dawson, C. T. A. Brown, and W. Sibbett, “Femtosecond pulse operation of a Tm,Ho-codoped crystalline laser near 2 µm,” Opt. Lett. **35**, 172-174 (2010).
8. A. A. Lagatsky, X. Han, M. D. Serrano, C. Cascales, C. Zaldo, S. Calvez, M. D. Dawson, J. A. Gupta, C. T. A. Brown, and W. Sibbett, “Femtosecond (191 fs) $NaY(WO_4)_2$ Tm,Ho-codoped laser at 2060 nm,” Opt. Lett. **35,** 3027-3029 (2010).
9. J. Zhang, K. F. Mak, S. Gröbmeyer, D. Bauer, D. Sutter, V. Pervak, F. Krausz, and O. Pronin, “Generation of 220 fs, 20 W pulses at 2 µm from Kerr-lens mode-locked Ho:YAG thin-disk oscillator,” *Conference on Lasers and Electro-Optics 2017* (Optical Society of America), paper SM1I.6.
10. E. P. Chicklis, C. S. Naiman, R. C. Folweiler, and J. C. Doherty, “Stimulated emission in multiply doped Ho^{3+}:YLF and YAG - A comparison,” IEEE J. Quantum Electron. **8**, 225-230 (1972).
11. K. L. Nash, R. C. Dennis, N. J. Ray, J. B. Gruber, and D. K. Sardar, “Absorption intensities, emission cross sections, and crystal field analysis of selected intermanifold transitions of Ho^{3+} in Ho^{3+}:Y_2O_3 nanocrystals,” J. Appl. Phys. **106**, 063117 (2009).
12. Y. Zhao, H. Yu, Z. Wang, H. Zhang, X. Xu, and J. Wang, “Direct investigation of inhomogeneous spectrum broadening in Nd^{3+}:$Gd_xY_{1-x}VO_4$ series crystals,” J. Opt. Soc. Am. B **30**, 1241-1247 (2013).
13. A. Agnesi, A. Greborio, F. Pirzio, G. Reali, J. A. Au, and A. Guandalini, “40-fs Yb^{3+}:$CaGdAlO_4$ laser pumped by a single mode 350-mW laser diode,” Opt. Express **20**, 10077-10082 (2012).
14. J. Ma, H, Huang, K. Ning, X. Xu, G. Xie, L. Qian, K. P. Lon, and D. Tang, “Generation of 30 fs pulses from a diode-pumped graphene mode-locked Yb:$CaYAlO_4$ laser,” Opt. Lett. **41**, 890-893 (2016).
15. P. O. Petit, J. Petit, P. Goldner, and B. Viana, "Inhomogeneous broadening of optical transitions in Yb: $CaYAlO_4$," Opt. Mater. **30**, 1093-1097 (2008).
16. Y. Wang, G. Xie, X. Xu, J. Di, Z. Qin, S. Suomalainen, M. Guina, A. Härkönen, A. Agnesi, U. Griebner, X. Mateos, P. Loiko, and V. Petrov, “SESAM mode-locked Tm:CALGO laser at 2 µm,” Opt. Mater. Express **6**, 131-136 (2015).
17. J. Q. Di, D. H. Zhou, X. D. Xu, C. T. Xia, W. Gao, H. R. Zheng, Q. L. Sai, F. Mou, and J. Xu, “Spectroscopic properties of Tm,Ho:$CaYAlO_4$ single crystal,” Cryst. Res. Technol. **49**, 446-451 (2014).
18. S. F. Gao, Z. Y. You, J. L. Xu, Y. J. Sun, and C. Y. Tu, “Continuous wave laser operation of Tm and Ho co-doped $CaYAlO_4$ and $CaGdAlO_4$ crystals,” Mater. Lett. **141**, 59-62 (2015).
19. J. Paajaste, S. Suomalainen, A. Härkönen, U. Griebner, G. Steinmeyer, and M. Guina, “Absorption recovery dynamics in 2 µm GaSb-based SESAMs,” J. Phys. D: Appl. Phys. **47**, 065102 (2014).
20. G. Rustad and K. Stenersen, “Modeling of laser-pumped Tm and Ho lasers accounting for upconversion and ground-state depletion,” IEEE J. Quantum Electron. **32**, 1645-1656 (1996).
21. N. K. Giri, D. K. Rai, and S. B. Rai, “White light upconversion emissions from Tm^{3+} + Ho^{3+} + Yb^{3+} codoped tellurite and germanate glasses on excitation with 798 nm radiation,” J. Appl. Phys. **104**, 113107 (2008).
22. J. H. Chung, J. H. Ryu, S. W. Mhin, K. M. Kim, and K. B. Shim, “Controllable white upconversion luminescence in Ho^{3+}/Tm^{3+}/Yb^{3+} co-doped $CaMoO_4$,” J. Mater. Chem. **22,** 3997-4002 (2012).
23. P. Loiko, P. Becker, L. Bohatý, C. Liebald, M. Peltz, S. Vernay, D. Rytz, J. M. Serres, X. Mateos, Y. Wang, X. Xu, J. Xu, A. Major, A. Baranov, U. Griebner, and V. Petrov, “Sellmeier equations, group velocity dispersion, and thermo-optic dispersion formulas for $CaLnAlO_4$ (Ln = Y, Gd) laser host crystals,” Opt. Lett. **42**, 2275-2278 (2017).
24. Y. Ishida, K. Naganuma, and H. Kamada, “Muti-sideband generation in a femtosecond Cr^{4+}:YAG laser,” Opt. Rev. **6**, 37-41 (1999).
25. Z. Sun, T. Hasan, F. Torrisi, D. Popa, G. Privitera, F. Wang, F. Bonaccorso, D. M. Basko, and A. C. Ferrari, “Graphene mode-locked ultrafast laser,” ACS Nano **4**, 803-810 (2010).
26. M. Schellhorn, D. Parisi, M. Eichhorn, and M. Tonelli, “Continuous-wave and Q-switched operation of a resonantly pumped Ho^{3+}:KY_3F_{10} laser,” Opt. Lett. **39**, 1193-1196 (2014).